



Universiteit  
Leiden  
The Netherlands

## **Spatio-temporal gene expression analysis from 3D in situ hybridization images**

Welten, M.C.M.

### **Citation**

Welten, M. C. M. (2007, November 27). *Spatio-temporal gene expression analysis from 3D in situ hybridization images*. Leiden Institute of Advanced Computer Science, group Imaging and Bio-informatics, Faculty of Science, Leiden University. Retrieved from <https://hdl.handle.net/1887/12465>

Version: Corrected Publisher's Version

License: [Licence agreement concerning inclusion of doctoral thesis in the Institutional Repository of the University of Leiden](#)

Downloaded from: <https://hdl.handle.net/1887/12465>

**Note:** To cite this publication please use the final published version (if applicable).

## Chapter 3

# Expression analysis of the genes encoding 14-3-3 gamma and tau proteins using the 3D digital atlas of zebrafish development

M.C.M. Welten<sup>1,2</sup>, A. Sels<sup>1,2</sup>, M.I. Van den Berg – Braak<sup>1</sup>, G.E.M. Lamers<sup>2</sup>, H.P. Spaik<sup>2</sup> and F.J. Verbeek<sup>1</sup>

1. Imagery and Media, Leiden Institute of Advanced Computer Science, Leiden University, Niels Bohrweg 1, 2333 CA Leiden, The Netherlands.
2. Section Molecular Cell Biology, Institute of Biology, Leiden University, Clusius Laboratory, Wassenaarseweg 64, 2333 AL Leiden, The Netherlands

Paper in preparation

## Case study Early zebrafish development

## ABSTRACT

The 14-3-3-protein family is a highly conserved family of small dimeric proteins, found in all eukaryotes. Extensive studies in yeast, plants, insects and vertebrates have shown that the 14-3-3 protein family members play a role in numerous cellular signaling processes, e.g. cell division, metabolism, apoptosis, and differentiation. Studies by Muslin et al. (1996) and Morrison et al. (1993) reveal functions for 14-3-3 in Raf phosphorylation and phosphoserine binding. Although the 14-3-3 proteins are ubiquitously expressed in all tissues, they are abundantly expressed in the vertebrate brain. Extensive studies of 14-3-3 expression patterns in mouse and rat brain show altered 14-3-3 protein levels in neurodegenerative diseases like Alzheimer's disease, Creutzfeld-Jakob disease and scrapie. Furthermore, the 14-3-3 proteins have been indicated to play an important role in several other neurological disorders such as epilepsy; and epithelial cancers such as breast and gastric cancer (reviewed by Dougherty and Morison, 2004). Recently, gene expression patterns of the genes encoding 14-3-3 isoforms in zebrafish were described by Besser et al. (2006). This research paved the way for a more complete, exact localization of zebrafish 14-3-3 gene expression patterns.

In this paper, we present an analysis of zebrafish 14-3-3  $\gamma$  and  $\tau$  isoforms, using whole mount fluorescent *in situ* hybridisation (FISH), *in situ* hybridisation (ISH) and TDR-3Dbase reconstruction software. From confocal laser scanning microscopy (CLSM) images as well as from serial sections, 3D reconstructions are obtained to analyze expression patterns of genes encoding 14-3-3, thereby using the 3D atlas of zebrafish development as a reference. The methods presented facilitate a more sensitive and precise spatiotemporal analysis of genes encoding 14-3-3  $\gamma$  and  $\tau$  isoforms during zebrafish embryonic development, and yield more gene expression domains at earlier stages than previously observed. Moreover, the methods are less time-consuming than those previously used. In future functional studies, the 3D reconstructions made with TDR-3Dbase reconstruction software allow an analytical approach to the gene expression domains.

**Keywords:** 14-3-3 proteins, fluorescent *in situ* hybridisation, 3D reconstruction, zebrafish brain development

## INTRODUCTION

The 14-3-3 protein family members are a highly conserved family of proteins, present in yeast, plants (Lu et al, 1994), insects (Swanson and Ganguly, 1992) and vertebrates (Koskinen et al. 2004 Watanabe et al. 1993; Wu et al. 2002). The name of the 14-3-3 proteins is derived from their migration position on DEAE cellulose chromatography and starch gel electrophoresis (Aitken et al. 1995). In *Xenopus*, 6 isoforms (Lau et al. 2006), in mammals 7 isoforms (Rosner and Hengstschlaeger, 2006) and in zebrafish, 11 isoforms are found. During vertebrate development, 14-3-3 proteins are mainly expressed in neural tissue and brain structures (Koskinen et al. 2004; Wu et al. 2002). Recent studies show that 14-3-3 proteins are involved in cancer and neurological disorders (reviewed by Dougherty and Morrison, 2004).

Both sequence and structure of the 14-3-3 proteins are remarkably conserved in all eukaryotes. Human 14-3-3  $\gamma$  protein shows 95% similarity with zebrafish 14-3-3  $\gamma$  protein; the sequence of the human 14-3-3  $\tau$  gene shows 76 % similarity with zebrafish 14-3-3  $\tau$  gene). The crystal structure of the 14-3-3 proteins shows that they are dimeric proteins. They are predominantly helical and form a negatively charged groove. The interior of this groove consists of almost invariant amino acids in all 14-3-3 family members (Aitken, 1996) and forms a phosphoprotein-binding surface that interacts with a large amount of cellular proteins (Dougherty and Morrison, 2004). 14-3-3 binding of a target protein may (i) protect it from dephosphorylation or proteolysis, (ii) modulate its activity, (iii) alter its ability to interact with other partners, (iv) modify its cytoplasmic/nuclear partition, or (v) serve as an adapter or scaffold to bridge proteins (Rosner and Hengstschlaeger, 2006). The 14-3-3 protein family is involved in numerous cellular pathways, such as metabolism, cell cycle, differentiation, signalling and apoptosis (Dougherty and Morrison, 2004). Therefore, it is not surprising that 14-3-3 proteins are involved in pathogenesis and progression of neurological disorders and cancer, where altered regulation of 14-3-3 proteins may influence the activity of binding partners. Also, loss of anti-apoptotic functions and tumor suppressor functions of 14-3-3 may lead to progression of certain cancers (reviewed by Dougherty and Morrison, 2004).

### *14-3-3 $\gamma$ isoform*

In vertebrates, 14-3-3  $\gamma$  isoforms are expressed in the developing and adult brain. During *Xenopus* embryonic development, the 14-3-3  $\gamma$  isoform shows variable levels of expression in cranium and central nervous system. Extensive studies with 14-3-3  $\gamma$  specific morpholino injections in 2-cell stage *Xenopus* embryos result in reduction and even inhibition of eye development (Lau et al. 2006). The mechanism of this inhibition of eye development is still unknown. In rat embryos, expression of the gamma isoform is found throughout the brain and spinal cord (Watanabe et al, 1994). In zebrafish two highly similar isoforms of the 14-3-3  $\gamma$  isoform are found (called  $\gamma 1$  and  $\gamma 2$ ). During embryonic development of zebrafish, expression of the gene encoding the 14-3-3  $\gamma 1$  isoform was found in telencephalon, diencephalon, the tegmentum of the mesencephalon and the cranial ganglia (Besser et al. 2006). However, it is likely that the probes used in the previous study are not able distinguish between the two representatives of the 14-3-3  $\gamma$  gene.

### *14-3-3 $\tau$ isoform*

Recent studies show that 14-3-3  $\tau$  isoform is involved in vertebrate brain development, and that it remains expressed during adulthood. In *Xenopus* embryos, 14-3-3  $\tau$  isoforms were abundantly expressed in trunk, skeletal myotomes, and tail fin regions. Injections with antisense  $\tau$  specific morpholinos in 2 cell stage embryos, led to severe gastrulation defects (Lau et al. 2006).

In mouse and rat embryos, 14-3-3  $\tau$  protein expression is found throughout the brain. At postnatal stages however, it is mostly found in the white matter and in the hippocampus (Baxter et al. 2002, Watanabe et al. 1994). In zebrafish embryos, two highly similar  $\tau$  isoforms (called  $\tau_1$  and  $\tau_2$ ) are found. The 14-3-3  $\tau_1$  isoform shows diffuse expression in substructures of the eye and several brain structures (Besser et al. 2006). However, for both the zebrafish  $\tau_1$  and  $\tau_2$  isoforms it is likely that the probes used in previous experiments could not distinguish between the two representatives of these genes.

### *14-3-3 and neurological disorders*

Analysis of 14-3-3 isoforms in the brain of rat embryos showed that the isoforms are involved in neuronal proliferation, migration and differentiation (Watanabe et al. 1993, 1994). Experiments in mouse and rat reveal altered 14-3-3 protein levels in the brain, in epilepsy (Schindler et al. 2006) and scrapie (Baxter et al. 2002). In humans suffering from Creutzfeldt –Jakob disease, Alzheimer’s disease and multiple sclerosis, 14-3-3 proteins are released into the cerebrospinal fluid as a consequence of extensive destruction of the brain, e.g. destruction of neurons. The presence of 14-3-3  $\gamma$  proteins in cerebrospinal fluid is used as a diagnostic marker for neurodegenerative disorders like Alzheimer’s disease (Fountoulakis et al. 1999; Van Everbroek et al. 2005), Creutzfeldt Jakob disease (Shiga et al. 2006) and multiple sclerosis (Bartosik and Archelos 2004).

The aim of our study is to accurately localize gene expression of 14-3-3 isoforms in the developing zebrafish brain as well as in other structures.

### *Neurogenesis*

In adult mammals, production of new neurons – i.e. adult neurogenesis – is found in two restricted areas in the central nervous system: in a particular region of the hippocampus and in the lateral ventricular zones, from which newly formed neurons migrate towards the olfactory bulb (Fig.1). In teleost fish however, numerous brain regions are able to form new neurons, also during adulthood (Zupanc et al, 2005). In zebrafish, neuronal proliferation zones are found in almost all brain divisions (Fig.1), including the olfactory bulb and the dorsal telencephalon - where a region was found, presumably homologous to the hippocampus in mammals (Zupanc et al. 2005). This might implicate a different role for 14-3-3 proteins during embryonic and adult neurogenesis. In addition, identification of cellular mechanisms that enable formation of new neurons in almost all regions of the adult fish brain might provide a clue for therapeutic approaches for the treatment of neurodegenerative diseases in the future.

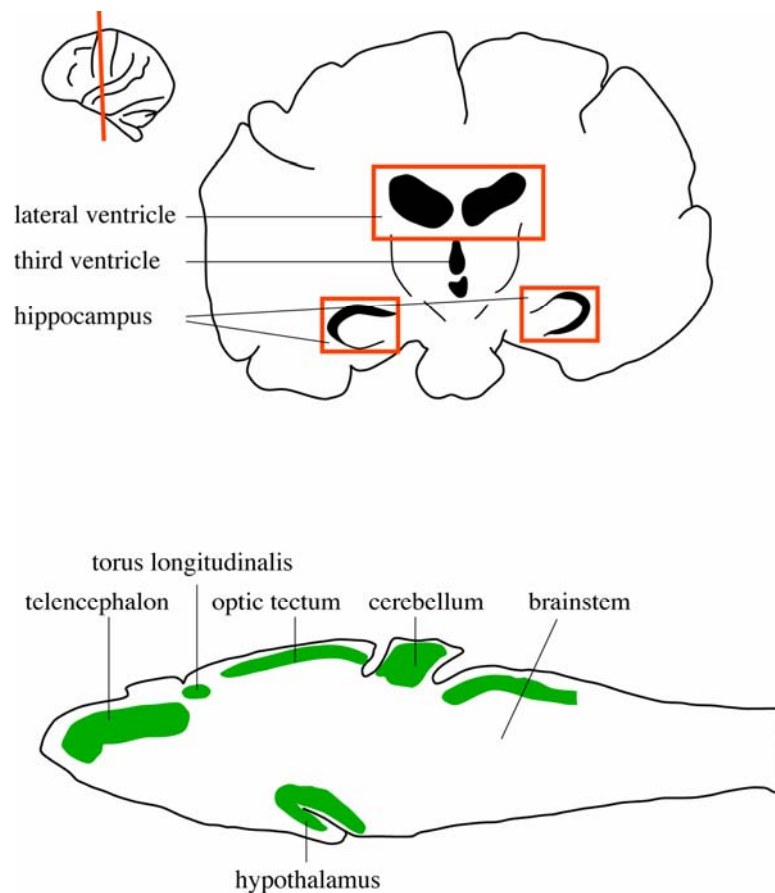


**Fig.1**, upper panel: author's impression of zones of adult neurogenesis in the human brain, boxed areas.

Lower panel: author's impression of the zebrafish brain. Zones of adult neurogenesis are marked in green (after Zupanc et al. 2005; Mueller and Wulliman, 2005)

### *3D atlas of zebrafish development*

In our research group, we have developed a 3D atlas of zebrafish development. In addition, a zebrafish gene expression database is under construction (Verbeek et al. 2000; <http://bio-imaging.liacs.nl>). Results of experiments can be stored in this database.

Gene expression data are produced using the ZebraFISH protocol (Welten et al. 2006) to facilitate 3D imaging with confocal laser scanning microscopy (CLSM). These 3D images can be processed with TDR-3D software to make 3D reconstructions, thus providing a schematic modelling of the structures and patterns observed in the CLSM images. The gene expression patterns can be mapped on anatomical structures, using the 3D atlas of zebrafish development as a reference. In this way, more insight in the spatial relationships of gene expression domains is obtained (Verbeek et al. 2002, Verbeek et al. 2004).

In recent years, the zebrafish has proven to be an excellent model system to study human disorders, amongst these, cancer and neurological diseases (Stern and Zon, 2003). Gene expression patterns for the zebrafish 14-3-3 isoforms were described in generic context. (Besser et al. 2006). However, gene expression patterns in zebrafish were not yet exactly localized. Given the involvement of 14-3-3 proteins in development and human

disorders, it is important to accurately map the gene expression patterns of 14-3-3 isoforms in zebrafish brain development. So as to pave the way for further functional analyses of the 14-3-3 isoforms and their involvement in diseases.

In this study, we present a three-dimensional analysis of gene expression for genes encoding the 14-3-3 $\gamma$  and  $\tau$  isoforms in the zebrafish embryo using fluorescent *in situ* hybridisation (zebraFISH) (Welten et al. 2006) during subsequent stages of development. *In situ* hybridisation (ISH) (Thisse et al. 2004) is used in parallel as a control for the procedure. In addition, ISH stained embryos are processed for serial sectioning. 3D images from FISH stained embryos are obtained by CLSM and these images are used to produce 3D reconstructions with TDR-3Dbase software (Verbeek et al. 1995). Moreover, 3D models are obtained in the same manner from serial sections. The techniques presented in this study provide an accurate spatiotemporal characterization of gene expression patterns encoding the 14-3-3 proteins in the developing zebrafish. Furthermore, the 3D techniques allow more analytical approach in future functional studies.

## MATERIALS AND METHODS

### *Obtaining gene expression data*

Zebrafish were maintained under standard conditions (<http://zfin.org>) in our facilities. Zebrafish embryos were harvested and staged to 18, 24, 36 and 48 hours post fertilization (hpf) as described by Kimmel et al. (1995) and processed for *in situ* hybridization (zebraFISH; Welten et al, 2006) and *in situ* hybridization (ISH; Thisse et al. 2004). Cloning and antisense RNA probe synthesis of the genes encoding 14-3-3  $\gamma$ 1 and  $\tau$ 1 used in this study have been described by Besser et al (2006). Our results are based on these  $\gamma$ 1 and  $\tau$ 1 probes. From now on, we will refer to these probes as 14-3-3  $\gamma$  and  $\tau$ . Supplementary information concerning genes encoding zebrafish 14-3-3  $\gamma$ 1 and  $\tau$ 1 proteins, ZFIN gene name and genomic location are described by Besser et al (2006).

### *Microscopy and imaging*

Confocal images were acquired according to a standard protocol (Welten et al., 2006) using a Leica TCS/SP DM IRBE confocal laser-scanning microscope equipped with an Ar/Kr laser. Excitation of the used fluorophores (Cy3 and SYTOXGreen) resulted in emission in a red and green spectrum; detected with separate laser channels (Kr and Ar, respectively). All images were obtained with a 10x plan apo lens (NA 0.24). For every image, photo multiplying tube (PMT) gain and offset were optimised to reduce the signal to noise ratio. Images were saved as two-channel multiple TIFF files. Images of ISH-stained embryos were acquired using a Leica MZFL-III12 stereomicroscope equipped with a Leica DC 500 digital camera.

### *Tissue sectioning*

After ISH, whole mount embryos were overstained for 3 days in NBT/BCIP staining solution (Roche). Overstained embryos were embedded in Technovit 7100 (Heraeus Kulzer GmbH, Wehrheim, Germany). Sagittal sections of 4  $\mu$ m were cut on a Leica Ultracut E 388542 microtome. From the serial sections, 3D reconstructions were made as previously described (Verbeek, 2000).

### *3D reconstructions*

From the 3D images produced with CLSM, 3D reconstructions were made using TDR-3Dbase with a Wacom LCD graphical tablet. To annotate gene expression patterns in relation to the anatomical structures, the 3D reconstructions were compared with corresponding 3D embryos from the 3D atlas of zebrafish development (<http://bio-imaging.liacs.nl.html>).

As a reference for the annotation of brain structures, *otx2* and *pax2.1* and neurogenin-1 were used as molecular markers for diencephalon, mesencephalon, optic stalk and cranial ganglia in zebrafish (Welten et al. 2006). Additional anatomical and molecular data for were extracted from literature (cranial ganglia: Holzschuh et al. 2005, Wilson et al. 2007; anatomy: Mueller and Wulliman, 2005) and [www.zfin.org](http://www.zfin.org).

## RESULTS

### *14-3-3 $\gamma$ and $\tau$ expression patterns*

In table 1 and 2, a summary of expression patterns for genes encoding 14-3-3  $\gamma$  and  $\tau$  proteins is given. Gene expression domains are compared to those described by Besser et al (2006).

However, the application of ZebraFISH yielded more gene expression patterns, and at earlier stages than those found in previous studies. These results were consistent after repeating the experiments, and for almost all hybridized embryos.

Likewise in the study of Besser et al., it is expected that the used probes are not able to distinguish the difference between the two different representatives of the isoforms. From the 3D reconstructions no conclusive evidence could be produced.

### *14-3-3 $\gamma$*

Our FISH detection method yielded more expression pattern domains for genes encoding 14-3-3  $\gamma$  than described in previous experiments. Supplementary to the patterns described by Besser et al (2006), application of the zebraFISH protocol detected more gene expression domains and at earlier stages. These gene expression domains were consistent with those found in literature for other model systems (*Xenopus*: Lau et al., 2006; rat: Watanabe et al. 1993 and 1994). Our FISH experiments yielded clear expression signals for the  $\gamma$  isoform in the diencephalon, the optic stalk, the optic cup, the lens and the future heart region in 18 hpf (n=17, 88%) and 24 hpf embryos (n=12, 100%), as visible from Fig. 2A-D.

Moreover, the FISH detection revealed weak expression for 14-3-3  $\gamma$  in the optic tectum of the mesencephalon at 24 hpf (12/12, 100%) (Fig.2A, B, G and H).

At 48 hpf, a strong gene expression signal was localized in the heart region (n=5, 80%) (Fig.2C and D). These findings were constant over multiple FISH experiments. ISH experiments were carried out in parallel. Our FISH results were confirmed through serial sectioning of embryos after overstaining the ISH samples for 3-4 days (Fig.2 G and H). In previous studies, ISH detection yielded only weak expression signal in these structures at 24 hpf (Besser et al, 2006), and there was no conclusive evidence if this was background or weak signal. In table 1, gene expression patterns for 14-3-3  $\gamma$  are



summarized and compared with those found by Besser et al. Samples for imaging were taken at random from a staged batch.

3D modelling with TDR-3Dbase further established expression for 14-3-3  $\gamma$  in or adjacent to the otic vesicle, most likely in the future cranial ganglion VIII (Holzschuh et al. 2005, Wilson et al. 2007); cranial ganglion V (trigeminal ganglion), and the spinal cord neurons at 20 hpf (data not shown) and 24 hpf (Fig.2 B and D). 3D reconstruction also confirmed 14-3-3  $\gamma$  expression in the presumptive heart, the diencephalon and the optic stalk (Fig.2B). From 36 to 48 hpf, the total number of brain structures showing 14-3-3  $\gamma$  expression decreased. At 48 hpf, distinct expression patterns were only found in the cranial ganglia and the heart (Fig.2C and D).

**Fig.2 A:** FISH result for the gene encoding 14-3-3 $\gamma$  in a 24 hpf embryo. The picture is a confocal slice.

**C:** 14-3-3  $\gamma$  FISH result in a 48 hpf embryo; a so-called z-projection of the confocal image.

**A and C:** Gene expression is in red, i.e. the red channel of the CLSM image. The green depicts a background staining of the cell nuclei with SYTOX Green.

**2 B,D:** 3D reconstruction of the embryos shown in 2A and 2B respectively. Gene expression for 14-3-3  $\gamma$  is depicted in white. Both FISH images and 3D reconstruction clearly reveal gene expression patterns in otic vesicle (salmon), optic stalk (orange), cranial ganglia (light yellow), ganglion V (light orange), spinal cord neurons and heart primordium (red) at 24 and 48 hpf.

**2 E, F:** ISH results for 14-3-3  $\gamma$  at 24 and 48 hpf. Dorsal view; anterior is to the left.

**G:** 14-3-3  $\gamma$  ISH result at 24 hpf. Tissue section after overstaining, revealing gene expression in eye, tectum of the mesencephalon, cranial ganglia and around the otic vesicle.

**H:** 3D reconstruction of the embryo shown in 5A. In 5B, gene expression is displayed in relation to anatomical structures. 14-3-3  $\gamma$  gene expression domains are depicted in white. In all images, anterior is to the left, dorsal is to the top.

The findings after overstaining, tissue sectioning and 3D reconstruction of ISH results confirm our findings with FISH.

Abbreviations: ccv, common cardinal vein; cer, cerebellum; c g, cranial ganglia; c g V, fifth cranial ganglion; di, diencephalon; h, heart primordium; o v, otic vesicle; sp n, spinal cord neurons; tec, tectum of the mesencephalon; rh: rhombencephalon.

Color legend: gene expression: white; gill primordia: light green; cerebellum: blue; common cardinal vein: clear blue; diencephalon: orange; eye: salmon; lens: brown; heart primordium: red; otic vesicle: dark green; rhombencephalon: lilac; tectum (mesencephalon): purple; telencephalon: dark blue; 4<sup>th</sup> ventricle: clear blue.

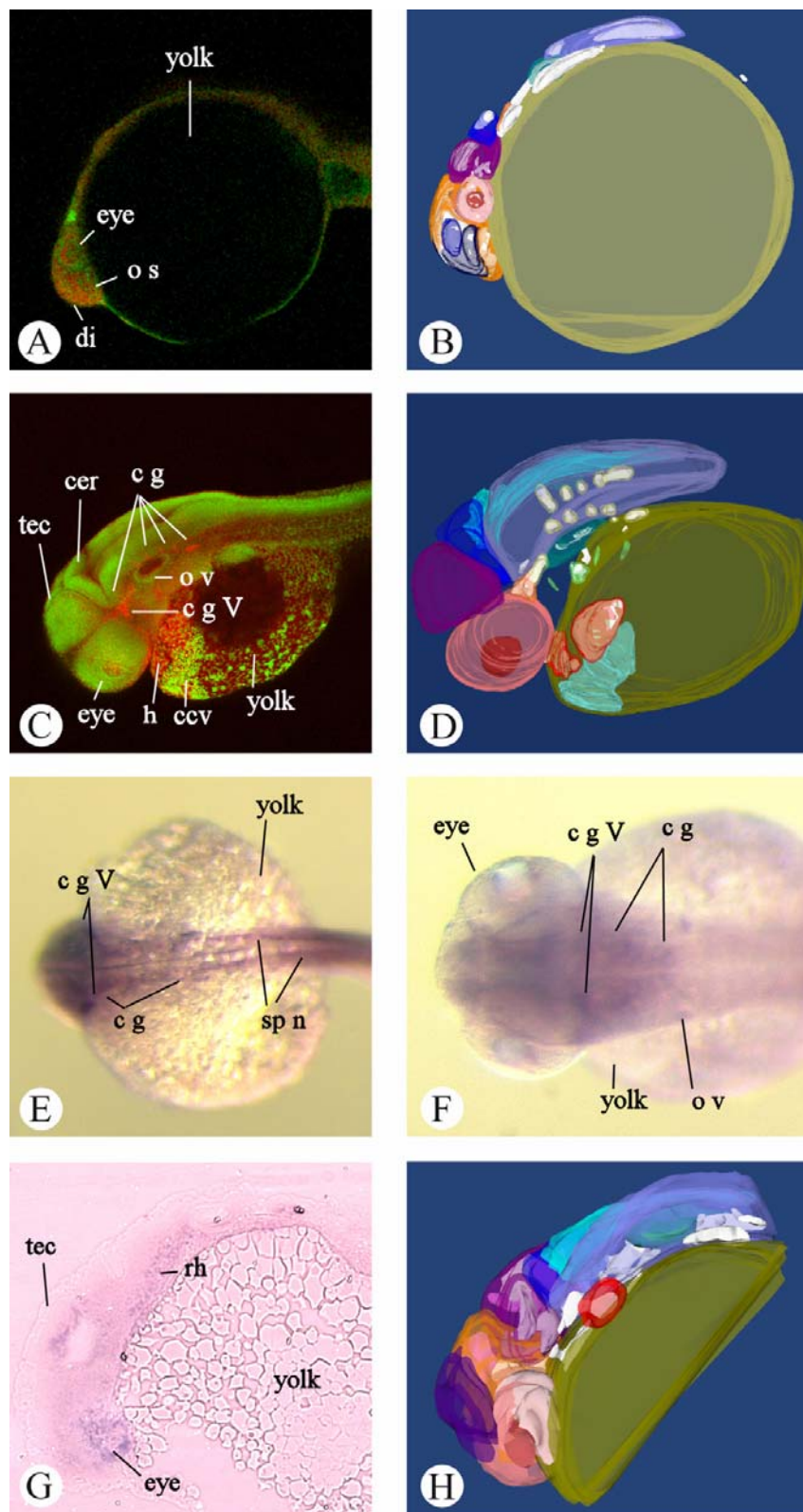


Fig. 2

*14-3-3  $\tau$* 

Our results show diffuse expression all over the brain structures and a prominent expression pattern in the in the optic cup and substructures of the eye; see Table 2 and Figure 3 A and B.

3D modelling for the  $\tau$  isoform reveals a distinct expression pattern in cranial ganglion V at 24 hpf (Fig. 5E, F). Furthermore, the  $\tau$  isoform displayed a more diffuse expression pattern throughout the brain structures from 20 hpf up to 48 hpf.

Two marker genes of brain development were used to verify and map our results: the *otx2* gene showed expression in diencephalon and mesencephalon (Mercier et al.1995), and *pax2.1* showed expression domains in the midbrain-hindbrain boundary, the optic stalk and the otic vesicle (Lun and Brand, 1998) (Fig. 4 A and B).

In figure 6, gene expression for 14-3-3  $\gamma$  and  $\tau$  in brain structures is compared over time.

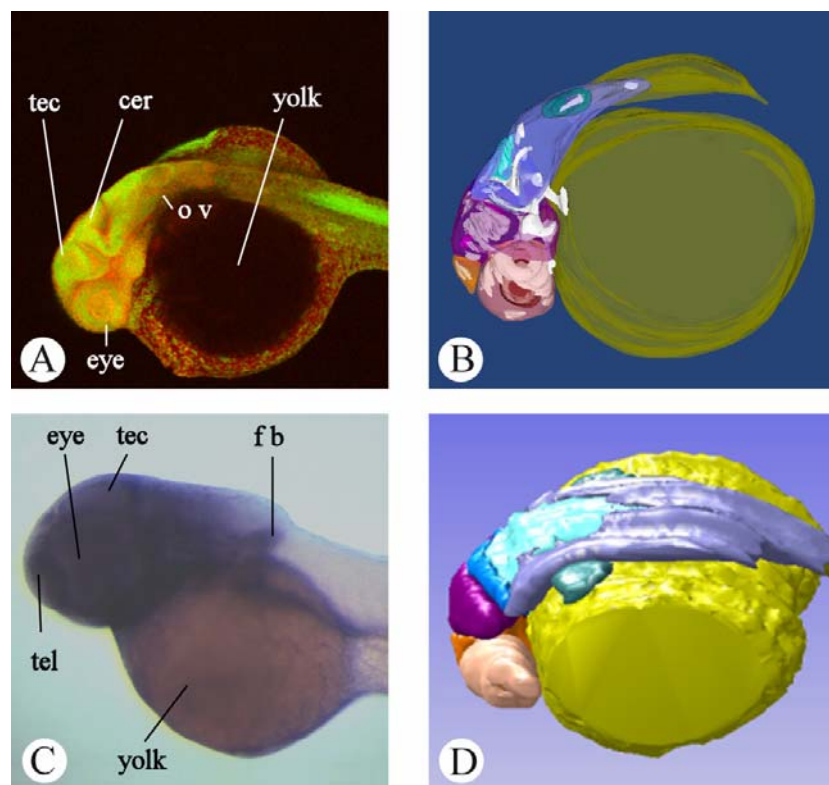


**Fig. 3 A:** 14-3-3  $\tau$  FISH result in a 24 hpf embryo; z-projection of a confocal image.

**B:** 3D reconstruction of the embryo shown in 3A. 14-3-3  $\tau$  gene expression (white) is visible in most brain structures.

**C:** Gene expression for 14-3-3  $\tau$  at 36 hpf, ISH detection.

**D:** Reference image from the 3D atlas, in the same orientation as the embryo in 3A and B.

Abbreviations: cer, cerebellum; fb: fin bud; o v, otic vesicle; tec, tectum of the mesencephalon; tel: telencephalon. In all images, anterior is to the left, dorsal is to the top.

Color legend: gene expression: white; cerebellum: blue; diencephalon: orange; eye: salmon; lens: brown; otic vesicle: dark green; rhombencephalon: lilac; tectum (mesencephalon): purple; 4<sup>th</sup> ventricle: clear blue.

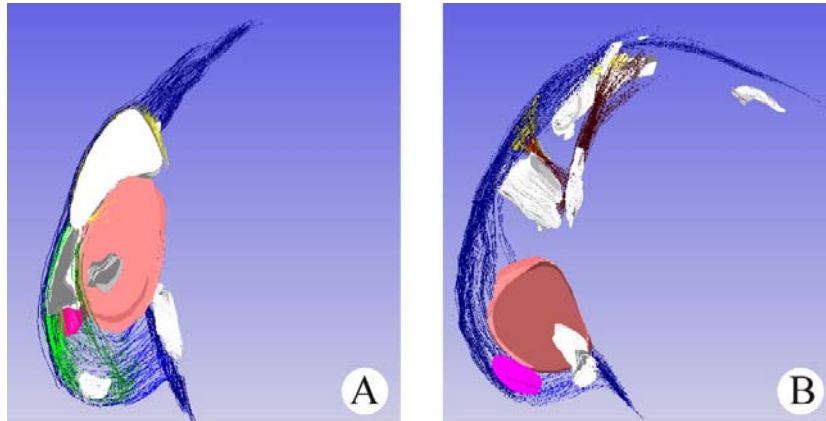


**Fig.4 A, B:** 3D reconstructions of *pax2* (4A) and *otx2* (4B) expression domains at 24 hpf, used as a reference for the brain structures.

In all images, anterior is to the left, dorsal is to the top. Color legend: gene expression: white; optic cup: salmon; embryo outline: dark blue.

**Table 1.** Summary of gene expression patterns found with ISH (Besser et al, 2006) and FISH (this study) for the 14-3-3  $\gamma$ 1 isoform

<b>Probe</b>	<b>ISH 18 hpf (Besser et al, 2006)</b>	<b>FISH 20 hpf n=17</b>
$\gamma$	diencephalon  spinal cord neurons	diencephalon optic stalk mesencephalon tectum tegmentum cranial ganglia cranial ganglion V spinal cord neurons otic vesicle/ cranial ganglion VIII? eye retina and lens heart primordium
	<b>ISH 24 hpf (Besser et al, 2006)</b>	<b>FISH 24 hpf n=12</b>
	telencephalon diencephalon  mesencephalon  tegmentum rhombencephalon cranial ganglia  spinal cord neurons otic vesicle	telencephalon diencephalon optic stalk mesencephalon tectum tegmentum rhombencephalon cranial ganglia cranial ganglion V spinal cord neurons otic vesicle/cranial ganglion VIII? eye retina and lens heart primordium
	<b>ISH 36 hpf</b>	<b>FISH 36 hpf n=2</b>
	no data available	diencephalon rhombencephalon cranial ganglia cranial ganglion V otic vesicle/cranial ganglion VIII? eye retina heart primordium
	<b>ISH 48 hpf (Besser et al, 2006)</b>	<b>FISH 48 hpf n=11</b>
	diencephalon hypothalamus mesencephalon tegmentum rhombencephalon  cranial ganglion V otic vesicle	diencephalon   rhombencephalon cranial ganglia cranial ganglion V otic vesicle/cranial ganglion VIII? heart

**Table 2.** Summary of gene expression patterns revealed by ISH (Besser et al. 2006) and FISH (this study).

$\tau 1$	ISH 18 hpf (Besser et al, 2006)	FISH 20 hpf n=11
	optic cup	telencephalon diencephalon mesencephalon tectum rhombencephalon cranial ganglion V spinal cord neurons eye lens retina boundary
	ISH 24 hpf (Besser et al, 2006)	FISH 24 hpf n=42
	telencephalon  mesencephalon tectum rhombencephalon ventricular zone  spinal cord neurons eye lens retina boundary	telencephalon  diencephalon  mesencephalon tectum rhombencephalon fourth ventricle zone cranial ganglion V spinal cord neurons eye lens retina boundary
	ISH 36 hpf (Besser et al, 2006)	FISH 36 hpf n=12
	no data available	telencephalon diencephalon mesencephalon tectum rhombencephalon cranial ganglion V spinal cord neurons eye retina boundary
	ISH 48 hpf (Besser et al, 2006)	FISH 48 hpf n=53
	diencephalon  rhombencephalon cranial ganglion V otic vesicle eye retina fin buds /liver	telencephalon diencephalon mesencephalon tectum rhombencephalon cranial ganglion V  eye retina boundary

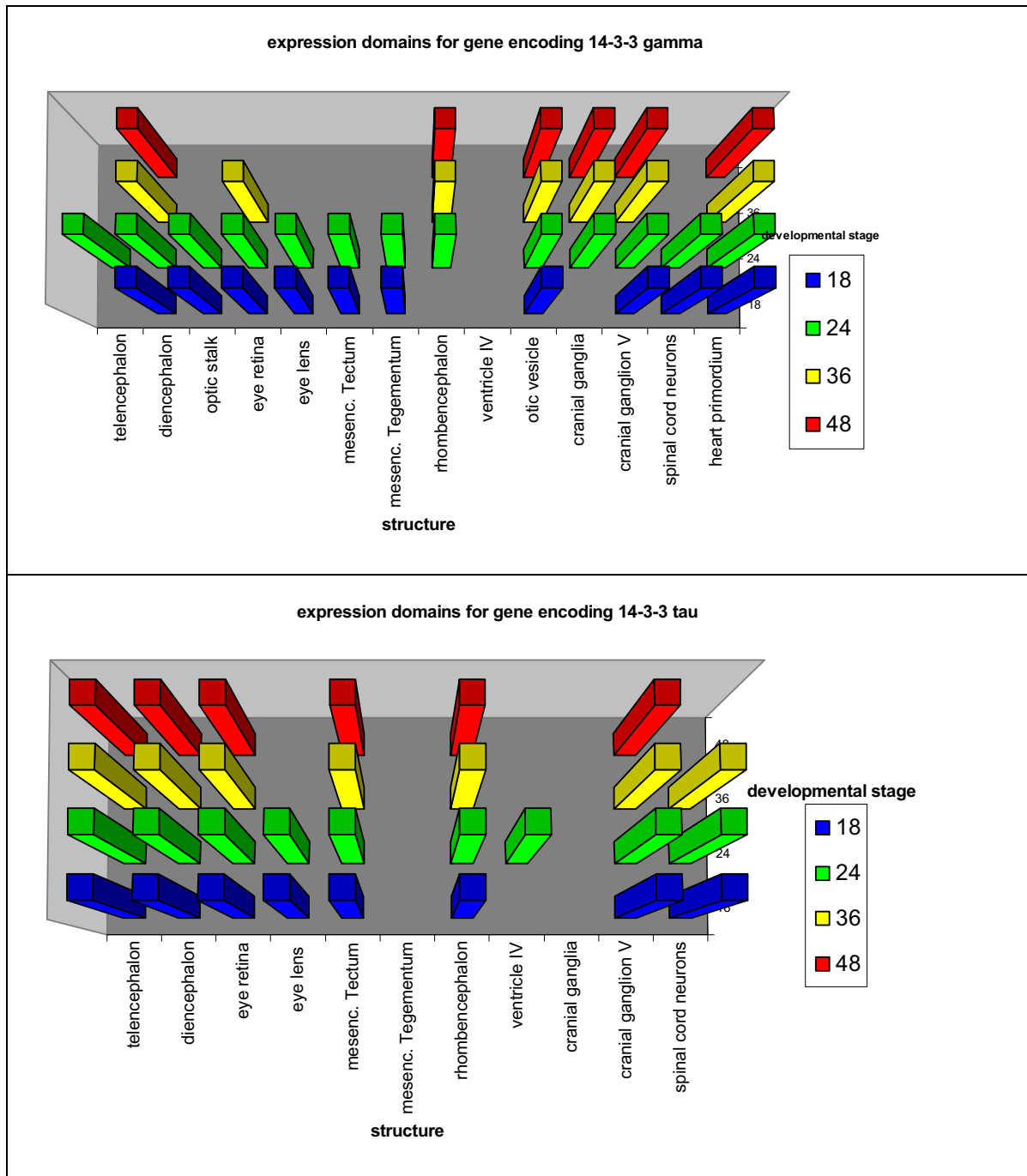


**Fig. 6.** Diagrams showing the total number of gene expression domains for 14-3-3  $\gamma$  (upper panel) and  $\tau$  (lower panel) in developmental time series from 18 up to 48 hpf. For the  $\gamma$  isoform, the number of expression domains decreases over time, where 14-3-3  $\tau$  remains more evenly expressed over brain structures at the same stages.

## DISCUSSION

The gene expression patterns revealed by zebraFISH confirm findings from a previous study (Besser et al. 2006) but in addition, due to higher sensitivity of the method, much more gene expression domains were found; especially at earlier stages of development. At 24 and 48 hpf, a strong signal for the gene encoding 14-3-3  $\gamma$  was observed in the dorsal region of the diencephalon and in the retina and lens. The Tyramide Signal Amplification (TSA) method used in our study is an amplification method, based upon the patented catalyzed reporter deposition (CARD) technology using derivatized tyramide. In the presence of hydrogen peroxide, immobilized Horse Radish Peroxidase converts the labeled tyramide substrate into a short-lived, extremely reactive intermediate that rapidly reacts with and covalently binds to electron rich regions of adjacent proteins (Jowett, 2001; Zaidi et al. 2000). Therefore, it is more sensitive than the Alkaline Phosphatase (AP) detection used in the in situ hybridisation. So, regions that show only a weak gene expression for 14-3-3  $\gamma$  in the AP detection might yield a stronger signal with TSA detection.

In our study, gene expression patterns for 14-3-3  $\gamma$  were found in substructures of the eye at 24 hpf. Expression patterns for the  $\gamma$  isoform in the eye are described for lower vertebrates such as the rainbow trout (Koskinen et al. 2004) and *Xenopus* (Lau et al. 2006). *Xenopus* embryos injected with 14-3-3  $\gamma$  specific morpholino show inhibition of eye development (Lau et al. 2006). Though little is known about the role of 14-3-3 isoforms in eye development, recent studies show that 14-3-3  $\gamma$  and  $\tau$  are expressed in the adult chick retina (Pozdeyev et al. 2006) and rat retinal ganglion cells, and play a role in maintaining these cells (Ivanov et al. 2006).

In mouse and rat embryos (embryonic day 7.5 and 13 respectively), expression of the 14-3-3  $\gamma$  protein is found in the ventral horn of the spinal cord, in the dorsal root ganglia and in the 5<sup>th</sup> ganglion (Baxter et al. 2002, Watanabe et al. 1993, 1994); our data for the gene encoding 14-3-3  $\gamma$  in zebrafish show expression in by and large the same structures. 14-3-3 expression was described in the neural crest of the rainbow trout (Koskinen et al. 2004). This also corresponds with our findings, since the neural crest has a broad developmental potential and gives rise to many cell types such as glial neurons (Wolpert, 2002).

Our FISH results show hybridization in the future heart region at 20-24 hpf embryos, and in the heart at 48 hpf. After overstaining with the AP detection method, serial sections from ISH stained embryos displayed weak but distinct gene expression patterns in the same region, confirming our FISH results. Interestingly, for rat and humans, 14-3-3  $\gamma$  has been indicated to play a role in heart disorders (He et al. 2006; Horie et al. 1999).

In our experiments, the gene encoding 14-3-3  $\tau$  shows diffuse expression throughout the brain from 20 up to 48 hpf. Prominent expression is found in the lens, the outer boundary of the retina and the spinal cord neurons from 20 somites up to 36 hpf in 92 % of the hybridized embryos at these stages (60/65, n = 65). Expression patterns were also found in telencephalon, diencephalon and mesencephalon (in the optic tectum) from 20 somites up to 48 hpf, in 95% of all hybridized embryos (106/111, n= 111). Besser et al. (2006) also describe gene expression for 14-3-3  $\tau$  expression in the pectoral fins the liver at 48 hpf, though this expression is very weak and might be an artifact. We found no FISH and ISH signal for this structure. No distinct FISH and ISH signal could be found in the liver.

In *Xenopus* embryos, the  $\tau$  isoform was expressed over the body surface, and later on in



the posterior trunk, tail fin region and in the skeletal myotomes (Lau et al. 2006). The latter might be a result of a difference in projection of the results. The pattern shown in Fig. 3 (Lau et al. 2006) is a 2D image. 3D reconstruction might reveal that the gene expression pattern found in the skeletal myotomes, is also located in the spinal cord neurons, as found in other vertebrates (Baxter et al.2002; Besser et al. 2006). The expression pattern of genes encoding 14-3-3  $\tau$  in zebrafish is consistent with gene and protein expression patterns found in mouse and rat embryos.

In the different model species, gene and protein expression patterns for 14-3-3  $\gamma$  and  $\tau$  are described either from the onset of neurulation up to subdivision of the prosencephalon into telencephalon and diencephalon (Baxter et al.2002, Watanabe et al. 1993 and 1994), or at later developmental stages (Besser et al.2006, Lau et al.2006), after completion of the five brain subdivisions.

Though our analysis portrays that the expression patterns for genes encoding zebrafish 14-3-3  $\gamma$  and  $\tau$  are found in the same structures as their orthologues described in the higher vertebrates, it might be interesting to compare gene expression at even earlier stages of zebrafish brain development. From extensive studies it is also evident that the 14-3-3 isoforms remain expressed in a wide variety of tissues and organs during adulthood (Bartosik and Archelos 2004, He et al. 2006, Horie et al. 1999, Kawamoto et al. 2006, Shiga et al. 2006).

In summary, the ZebraFISH and 3D reconstruction methods used in our study enabled a fast and precise localization of expression patterns of genes encoding 14-3-3  $\gamma$  and  $\tau$  in the zebrafish. Overstaining and tissue sectioning of ISH samples confirmed our FISH results. The gene expression patterns found in our study were consistent with those described for other model species (Koskinen et al. 2004; Lau et al. 2006; Watanabe et al. 1993 and 1994) and those described by Besser et al (2006). Our study also demonstrates that 3D analysis based on the 3D atlas of zebrafish development as a reference, provides an accurate localization of the genes encoding 14-3-3  $\gamma$  and  $\tau$  isoforms.

### *Conclusions and future work*

In this study, we present a 3D analysis of the genes incoding 14-3-3  $\gamma$  and  $\tau$  in several structures of the zebrafish brain and the developing central nervous system, in time series of early embryonic development. The 3D reconstructions, composed from CLSM images as well as from serial sections, provide detailed information on the spatial relations of the gene expression patterns during zebrafish brain development. Moreover, 3D reconstruction of 14-3-3 isoforms allows an analytical approach for functional analysis in the future. The spatial and temporal (i.e., during subsequent stages of embryonic development) analysis of 14-3-3 gene expression data and the techniques presented in this study, further facilitate studies of 14-3-3 family members in zebrafish development and in relation to in human disorders. For a more accurate localization of the genes encoding 14-3-3  $\gamma$  and  $\tau$ , colocalization experiments can be carried out with markers for cranial and lateral line ganglia. Also, timing of zebrafish 14-3-3 gene expression can be compared with other model species, using data acquisition methods.

## ACKNOWLEDGEMENTS

This project is partially supported by the Netherlands Research Council through the BioMolecular Informatics programme of Chemical Sciences (grant number #050.50.213) and by a BSIK project (Cyttron) from the Dutch Ministry of Economic Affairs (H.P.S). The authors would like to thank Dr. Jeroen Bakkers, who kindly donated *otx2* and *pax2* probes and Jeroen Korving and Merijn de Bakker for their helpful advice. The authors also would like to thank M. Brittijn for his help with the figures.

